



ERNEST ORLANDO LAWRENCE BERKELEY NATIONAL LABORATORY

Plasma Guiding and Wakefield Generation for Second Generation Experiments

W. Leemans, C.W. Siders, E. Esarey, N. Andreev,
G. Shvets, and W.B. Mori
**Accelerator and Fusion
Research Division**

March 1996
Submitted to
*IEEE Transactions on Nuclear
and Plasma Sciences*



REFERENCE COPY
Does Not
Circulate

Bldg. 50 Library.

Copy 1

LBL-38316

DISCLAIMER

This document was prepared as an account of work sponsored by the United States Government. While this document is believed to contain correct information, neither the United States Government nor any agency thereof, nor the Regents of the University of California, nor any of their employees, makes any warranty, express or implied, or assumes any legal responsibility for the accuracy, completeness, or usefulness of any information, apparatus, product, or process disclosed, or represents that its use would not infringe privately owned rights. Reference herein to any specific commercial product, process, or service by its trade name, trademark, manufacturer, or otherwise, does not necessarily constitute or imply its endorsement, recommendation, or favoring by the United States Government or any agency thereof, or the Regents of the University of California. The views and opinions of authors expressed herein do not necessarily state or reflect those of the United States Government or any agency thereof or the Regents of the University of California.

Plasma Guiding and Wakefield Generation for Second Generation Experiments*

W. Leemans, C. W. Siders¹, E. Esarey², N. Andreev³, G. Shvets⁴, and
W. B. Mori⁵
Center for Beam Physics
Lawrence Berkeley National Laboratory
University of California
Berkeley, California 94720

IEEE Transactions on Nuclear and Plasma Sciences

March 1996

* This work was supported by the Director, Office of Energy Research, Office of High Energy and Nuclear Physics, High Energy Physics Division, of the U. S. Department of Energy, under Contract No. DE-AC03-76SF00098.

¹ Physics Department, University of Texas at Austin, Austin, TX 78712

² Beam Physics Branch, Naval Research Laboratory, Washington, D.C. 20375-5320

³ High Energy Density Research Center, Russian Academy of Sciences, Moscow, 127412

⁴ Princeton Plasma Physics Laboratory, Princeton, NJ 08453

⁵ Physics Department, University of California at Los Angeles, CA 90024

Plasma Guiding and Wakefield Generation for Second Generation Experiments

Summary of the Working Group

W. Leemans, C.W. Siders, E. Esarey, N. Andreev, G. Shvets and W.B. Mori*

I. INTRODUCTION

The possibility of accelerating particles to high energy by laser generated, longitudinal electric fields in plasmas has been a subject of much interest [1]. The laser driver can either consist of a single large amplitude pulse (so called laser wake-field accelerator, LWFA), [1,2] a train of pulses with fixed spacing (so called plasma beat wave accelerator, PBWA) [1] or a train of pulses with variable spacing and pulse widths (so called resonant laser plasma accelerator, RLPA) [3]. First generation experiments using the PBWA [4] and LWFA [5] schemes, have shown that large accelerating gradients ($> 1\text{GeV/m}$) can be generated. For the PBWA, the acceleration of an externally injected electron beam has shown [4] that the phase velocity of these waves is close to the speed of light. Acceleration distances however have been limited to the diffraction distance (or Rayleigh length, Z_R) of the laser pulse, thereby limiting the energy imparted to the particle.

W. Leemans is with the Center for Beam Physics, Lawrence Berkeley National Laboratory, Berkeley, CA94720

C. W. Siders is with the Physics Department of the University of Texas at Austin

E. Esarey is with the Beam Physics Branch, Naval Research Laboratory, Washington, DC 20375-5320

N. Andreev is with the High Energy Density Research Center, Russian Academy of Sciences, Moscow, 127412.

G. Shvets is with the Princeton Plasma Physics Laboratory, Princeton, New Jersey 08453

W.B. Mori is with the Physics Department of the University of California Los Angeles, Los Angeles, CA90024

To extend the acceleration length for laser based schemes, optical guiding in plasmas has been proposed as a way of propagating a high power laser pulse over a distance of many Rayleigh lengths.[6-8] Analogous to optical fibers, the plasma density in a plasma guide is transversely tailored such that the plasma density profile has a minimum on axis, and hence a higher index of refraction on axis than off-axis.

Theory efforts on the possibility of using such plasma channels for high gradient laser driven acceleration have concentrated on the analysis of two different types of channels: a parabolic [7] and a hollow channel [8]. In the parabolic channel the wakefields arise from density bunching in the plasma at the channel axis. In the hollow channel wakefields are supported through surface currents at the channel edge. Analytic expressions exist which describe the wakefields generated by a nonevolving laser pulse in the three-dimensional (3D) linear regime and in the one-dimensional (1D) nonlinear regime. Certain properties of laser pulse propagation, such as the critical power for relativistic self-focusing, the critical depth for channel guiding, and the growth rates for various instabilities, can be described analytically. As an example, a self-consistent analysis of the coupled laser-plasma system was recently carried out to study instabilities of short laser pulses guided by a parabolic channel.[9] In general, the self-consistent problem of wakefield generation and laser pulse evolution requires numerical simulation.

Experimentally, guiding of laser pulses in a laser produced plasma channel has been studied in plasma channels produced with a two-pulse technique.[10] A first laser pulse was focused to a line focus with an axicon lens to produce a few cm long plasma, and subsequently heat it. The resulting hydrodynamic expansion led to a time-dependent density profile with a minimum on-axis. A second laser pulse was then injected into this channel with a variable delay time. For short delay times, the channel was fairly shallow and would support only the fundamental mode. For longer delay times, the channel was deeper and wider, thereby allowing higher order modes to propagate. Pulse propagation

over distances of up to 70 Rayleigh lengths (about 2.2 cm) of moderately intense laser pulses ($< 5 \times 10^{14}$ W/cm²), with pulse lengths much larger than the plasma period, was demonstrated in these experiments. Experiments will need to demonstrate the capability of such plasma channels to guide laser pulses with intensities on the order of 10^{18} W/cm² over macroscopic distances as well as controlled excitation of wakefields in such structures.

In light of the recent encouraging experimental results [4, 5] on generation of large amplitude wakefields in plasmas as well as on guiding of laser pulses in plasma channels [9], we have carried out a first order design study for a second generation plasma guiding and wakefield experiment. We have intentionally chosen to work out a design for which a) the laser driver has performance parameters currently achievable, b) the accelerating gradient in the experiment is larger than 1 GeV/m and c) exists over a distance comparable to a dephasing length or a pump depletion length (i.e. typically many Rayleigh lengths). In addition, we have kept in mind that the ensuing accelerating structure should have an acceptance large enough to be probed by an electron beam at an existing accelerator facility.

The first requirement has led us to express all relevant scaling laws in terms of laser system parameters: laser wavelength λ , peak power P and spot size r_s . The second requirement will be satisfied by operating the laser wakefield experiment at a plasma density which, for a given longitudinal pulse shape, is resonant with the pulse duration. Designs in which overall efficiency of laser-plasma coupling or net energy gain of the particle are the primary objective have not been carried out yet but will be the subject of future work. The third requirement will be satisfied by propagating the laser pulse inside a parabolic channel. As will be discussed in Section II, hollow channels may have favorable accelerating properties, however, creating such channels in the laboratory remains an important challenge.

The fourth requirement puts constraints on the ratio of laser beam size to plasma skin depth, $k_p r_s$. Since one of the design goals is to allow wakefield measurement with an available test particle beam, the width over which the longitudinal accelerating field is flat needs to be considered. For $k_p r_s$ close to unity, strong radial electric fields on the same order of the axial longitudinal field could lead to significant emittance degradation. Measurement of the wakefield properties in such a structure with a probe particle beam small compared to the width of the plasma wake, would put very stringent constraints on the minimum emittance required of the electron injector. For the design study we have chosen a laser spot size which results in a longitudinal gradient larger than 1 GeV/m and, at the same time, satisfies $k_p r_s > 1$ to minimize emittance degradation.

In Section II, we revisit the concept of laser guiding in plasmas, and summarize the conceptual differences between parabolic and hollow channels. Simple scaling laws are presented in Section III for the design of a laser wakefield experiment, from the perspective of the laser driver parameters: laser pulse energy, pulse length, repetition frequency. Two particular cases will be worked out which could address the following important experimental milestones with existing laser technology: a) guiding of a 10^{18} W/cm² laser pulse over a distance of several centimeters, b) generation of large amplitude wakefields in a plasma channel, c) measurement of phase space acceptance of the plasma wakes. Results of a numerical simulation for two design cases are presented in Section IV. We then briefly discuss possible schemes for generating plasma channels and optically diagnosing the wakefield structure in Section V. Important theoretical issues related to propagation of the laser pulse in the channel and the generation of the plasma wakefield will be discussed in Section VI, followed by a conclusion in Section VII.

II. PLASMA CHANNEL GUIDING: THEORY

A. Introduction

The optical guiding of laser pulses in plasmas over extended propagation distances (many Rayleigh lengths) can occur through a combination of effects: relativistic self-focusing,[11-16] preformed density channels [6-8,15] and plasma wave guiding [15,16]. These optical guiding mechanisms are based on the principle of refractive guiding. Refractive guiding can occur when the radial profile of the index of refraction, $\eta_R(r)$, exhibits a maximum on axis, i.e., $\partial\eta_R / \partial r < 0$. The index of refraction for a small amplitude electromagnetic wave propagating in a uniform plasma with density $n = n_0$ in the 1D limit is given by $\eta_R = ck / \omega = (1 - \omega_p^2 / \omega^2)^{1/2}$, where ω is the laser frequency and ω_p is the plasma frequency. For large amplitude waves, however, variations in the electron density and mass will occur, i.e.,[16]

$$\eta_R(r) \equiv 1 - \frac{\omega_p^2}{2\omega^2} \frac{n(r)}{n_0 \gamma(r)} \quad (1)$$

assuming $\omega_p^2 / \omega^2 \ll 1$. The leading order motion of the electrons in the laser field is the quiver motion $p_\perp = mca$ and, hence, $\gamma \equiv \gamma_\perp = (1 + a^2)^{1/2}$. Here, a^2 is related to the laser intensity I and wavelength λ by $2.8a_0^2 = 10^{18} \lambda^2 [\mu\text{m}] I [\text{W} / \text{cm}^2]$ (circular polarization).

The density profile can have contributions from a preformed density channel, e.g. $\Delta n_p = \Delta n r^2 / r_0^2$ where r_0 determines the curvature of the channel profile, or a plasma wave $\delta n \propto \delta n_0(r) \cos k_p \zeta$, where $\zeta = z - ct$ and $k_p = \omega_p / c$, i.e., $n = n_0 + \Delta n_p + \delta n$. In the limits $a^2 \ll 1$, $|\Delta n_p / n_0| \ll 1$ and $|\delta n / n_0| \ll 1$, the refractive index is given by

$$\eta_R(r) \equiv 1 - \frac{\omega_p^2}{2\omega^2} \left(1 - \frac{a^2}{2} + \frac{\Delta n_p}{n_0} + \frac{\delta n}{n_0} \right) \quad (2).$$

The last three terms on the right are responsible for the effects of relativistic optical guiding, density channel guiding, and plasma wave guiding, respectively.

An equation describing the evolution of the laser spot size r_s can be derived by analyzing the paraxial wave equation with an index of refraction given by Eqn. (2). Assuming the radial profile of the laser pulse is approximately Gaussian, $a^2 \propto \exp(-2r^2/r_s^2)$, the normalized laser spot size $R = r_s/r_0$ (r_0 = initial spot size) evolves according to [15,18-19]

$$\frac{d^2R}{dz^2} = \frac{I}{Z_R^2 R^3} \left[I - \frac{P}{P_c} - \frac{\Delta n}{\Delta n_c} R^4 + \frac{\delta n_0}{\Delta n_c} \frac{R^4}{R_p^2} \frac{\sin k_p \zeta}{(I + \alpha_p)^2} \right] \quad (3)$$

where $P \propto a^2 r_s^2$ is the laser power and is constant (independent of z) in the paraxial approximation, $Z_R = k r_0^2/2$ is the Rayleigh length, $R_p = r_p/r_0$ is the normalized plasma wave radius, $\alpha_p = r_s^2/2r_p^2$, and $P_c[\text{GW}] \equiv 17(\omega/\omega_p)^2$ is the critical power for self-focusing, [11-16].

The terms on the right side of Eqn.(3) represent vacuum diffraction, relativistic self-focusing, channel guiding, and the effects of the plasma wave, respectively. Note if $P = \Delta n = \delta n_0 = 0$, $r_s = r_0(1 + z^2/Z_R^2)^{1/2}$, which is the vacuum diffraction result. In the absence of a plasma wave, $\delta n_0 = 0$, the general condition [17] to guide (i.e., $r_s = \text{constant}$) a long, axially uniform pulse in a plasma is $P/P_c \geq 1 - \Delta n/\Delta n_c$. In the limit $\Delta n_p = \delta n_0 = 0$, it can be shown that the relativistic guiding of a long pulse occurs when the laser power satisfies $P \geq P_c$. On the other hand, in the limits $P/P_c \ll 1$ and $a^2 \ll 1$, it can be shown that a parabolic density channel $\Delta n_p = \Delta n r^2/r_0^2$ can guide a Gaussian laser pulse $a^2 \propto \exp(-2r^2/r_0^2)$ provided that the channel depth satisfies $\Delta n \geq \Delta n_c$, where $\Delta n_c = (\pi r_e r_0^2)^{-1}$ is the critical depth,[7,15] and $r_e = e^2/m_e c^2$ is the classical electron radius. This paper will be concerned with LWFA designs in which the laser pulse is guided primarily by a preformed plasma density channel, i.e., $\Delta n \approx \Delta n_c$ and $P/P_c \ll 1$. Note also that, because the resonant density is always greater than the critical density for beams with spotsizes greater or equal to the skin depth, guiding for a resonant pulse is always possible.

B. Parabolic and Hollow Channels for Particle Acceleration

While both parabolic channels (which are smooth on a scale of collisionless skin depth c / ω_p) and hollow channels (which we will use as a generic term for a channel with a sharp boundary even if the inside of the channel is not completely evacuated of plasma) are effective in guiding the laser pulse over distances longer than a Rayleigh length, their accelerating properties are rather different.

The hollow channel accelerator concept is an attempt to combine the benefits of plasma acceleration with some of the features of conventional radio-frequency (RF) accelerators. In an RF accelerator charged particles interact with an electromagnetic wave which can be either a standing TM mode of an RF cavity or an array of cavities, or a traveling mode in a slow-wave structure (for example, in a disc-loaded wave guide). Since a conventional accelerating cavity is relatively large in size, variation of the accelerating gradient is negligible across the beam which is important to maintain a small energy spread. Another attractive feature of a conventional accelerator stems from the fact that acceleration and transverse focusing are decoupled from each other. This is because the accelerating wave is electromagnetic, with almost equal radial component of the electric field and azimuthal component of the magnetic field. Therefore, the focusing force from the electric field and the defocusing force from the magnetic fields cancel to order $1/\gamma^2$, where γ is the relativistic Lorentz factor of the accelerated particle. Transverse focusing is accomplished by external magnets. A hollow channel configuration supports a weakly damped accelerating eigenmode which has a well defined frequency, independent of the radial position. Details on the linear analysis of the mode structure and dissipation rate as well as the results of fully nonlinear particle-in-cell (PIC) simulations can be found in Refs.[8, 18-19].

Briefly summarizing those results, an accelerating eigenmode has the structure of an electromagnetic TM mode, with non-vanishing E_z, B_ϕ, E_r components. The accelerating gradient is uniform (to order ω_p^2/ω_0^2) across the channel, and $B_\phi = E_r$ to the same order. Thus, the structure of the fields in the hollow channel accelerator closely resembles that of a conventional RF accelerator. Because of the uniformity of the accelerating gradient, the entire channel can be used for particle acceleration thereby increasing the acceptance of the accelerator.

Damping of the accelerating wake in a slab-like plasma channel of width $2b$ with wall thickness $\delta.b$ was estimated in Ref.[19] to be given by $\omega_{im} \approx 0.2\delta\omega_{ch}$ where $\omega_{ch} = \omega_p / \sqrt{1 + k_p b}$ is the wake eigenfrequency in a hollow channel with infinitely thin walls. Thus, if the wall thickness is comparable with the size of the channel, accelerating eigenwake is damped after one oscillation (which is confirmed by PIC simulations).

On the contrary, a smooth parabolic channel does not support global electromagnetic modes which are heavily damped. Instead, a laser pulse propagating through the channel excites electrostatic modes which oscillate at the local plasma frequency $\omega_p(r)$. The amplitude of the accelerating wake is proportional to the laser intensity. Therefore, to avoid appreciable energy spread one has to utilize a very limited (in transverse dimension) region of the wake so that the size of the beam $r_{beam} \ll r_s$.

Another potential problem with acceleration in a parabolic channel (as well as in the homogeneous plasma) is that the electrostatic wake does not have a magnetic component to balance the focusing electric field. Since an electron bunch has a finite length, the head and the tail of the bunch experience different focusing which can lead to effective emittance growth (see paper by Serafini, in these proceedings.).

The combination of a short betatron wavelength (because of the strong focusing in the electrostatic field) and spread in plasma frequency across the channel can also lead to

emittance growth and large energy spreads. One can estimate that for a 100 MeV electron beam accelerated by a gradient of 30 GeV/m in a 10^{18} cm^{-3} plasma, the betatron wavelength is $\lambda_\beta \approx 5 \times 10^{-2} \text{ cm}$. Therefore, an electron will execute about 20 betatron oscillations as it propagates through a centimeter of a plasma accelerator, sampling electric fields at various radial locations. Variation of the accelerating phase across the channel is roughly given by $\Delta\phi / (2\pi) \approx \Delta\omega_p / \omega_p$, where $\Delta\omega_p$ is proportional to density difference between $r = 0$ and $r = r_{\text{beam}}$. To assure that electron samples a well defined phase of the accelerating wake, a shallow parabolic channel has to be used, as in the second design example.

Overall, hollow channel offers superior accelerating properties but seem to be the hardest to realize in practice. It appears that before there is an established way of producing such channels, main experimental impetus has to be directed at production of shallow parabolic channels. Self-consistent calculations of the detailed three dimensional field structure in a parabolic channel need to be carried out in support of such experiments.

III. SCALING LAWS FOR GUIDING AND WAKEFIELD EXCITATION IN PARABOLIC CHANNELS

To design a second generation laser guiding and acceleration experiment we will start from a set of parameters which define a laser driver and utilize the linear 3D results previously published in the literature. We assume that the laser beam is focused transversely to a lowest-order Gaussian mode with mode size r_s , and that longitudinally it has an arbitrary pulse shape given by $f(\zeta)$. As a practical example we will take a Ti:Al₂O₃ laser system operating at a wavelength of 0.8 μm , which delivers a 50 fs long Gaussian laser pulse with a peak power of 5 TW. In the examples, two cases (A and B) with different laser spot size will be considered: case A (B) has $r_s = 17$ (42) μm .

For a given laser pulse shape, the required plasma density for resonant wakefield excitation can be found as follows. The laser pulse structure will generate a plasma wave according to the relation [17, 20-21]

$$\left(\frac{\partial^2}{\partial \zeta^2} + k_p^2\right) \frac{\delta n}{n_0} = \nabla^2 \frac{a^2}{2} \quad (4)$$

assuming $k_p^2 r_s^2 \gg 1$, $\delta n^2 / n_0^2 \ll 1$ and $a^2 \ll 1$. Separating out the longitudinal and transverse shape of the laser pulse we can write the square of the normalized vector potential as

$$a_L^2(\zeta, r) = a_0^2 f(\zeta) e^{-2(r/r_s)^2} \quad (5)$$

The solution to the driven harmonic oscillator equation (Eqn.(4)) can be written as

$$\begin{aligned} \frac{\delta n}{n} = & \frac{a_L^2(\zeta, r)}{2} + k_p \int_{\zeta}^{\infty} \sin(k_p(\zeta - \zeta')) \frac{a_L^2(\zeta', r)}{2} d\zeta' - \\ & \frac{1}{k_p} \int_{\zeta}^{\infty} \sin(k_p(\zeta - \zeta')) \left[\frac{1}{r} \frac{\partial}{\partial r} r \frac{\partial}{\partial r} \frac{a_L^2(\zeta', r)}{2} \right] d\zeta' \end{aligned} \quad (6)$$

Substituting Eqn. (5) into Eqn. (6) we obtain

$$\frac{\delta n}{n} = \frac{a_L^2(\zeta, r)}{2} + k_p \frac{a_0^2}{2} e^{-2(\tau/r_s)^2} \left[1 + \frac{8}{(k_p r_s)^2} \left(1 - 2\left(\frac{r}{r_s}\right)^2 \right) \right] \int_{-\infty}^{\infty} f(\zeta') \sin(k_p(\zeta - \zeta')) d\zeta' \quad (7).$$

Expanding the sine-function and assuming we are far away from the pump ($\zeta \rightarrow -\infty, f(\zeta) \rightarrow 0$) we get

$$\frac{\delta n}{n} = k_p \frac{a_0^2}{2} e^{-2(\tau/r_s)^2} \left[1 + \frac{8}{(k_p r_s)^2} \left(1 - 2\left(\frac{r}{r_s}\right)^2 \right) \right] \times \left[\sin(k_p \zeta) \int_{-\infty}^{\infty} f(\zeta') \cos(k_p \zeta') d\zeta' - \cos(k_p \zeta) \int_{-\infty}^{\infty} f(\zeta') \sin(k_p \zeta') d\zeta' \right] \quad (8)$$

The factors multiplying the sine and cosine functions are then the Fourier cosine and sine transforms of the longitudinal shape function respectively. Rewriting the difference in the form $A \sin(k_p \zeta + \delta)$ and converting back to time and frequency units we find

$$\frac{\delta n}{n} = k_p \frac{a_0^2}{2} e^{-2(\tau/r_s)^2} \left[1 + \frac{8}{(k_p r_s)^2} \left(1 - 2\left(\frac{r}{r_s}\right)^2 \right) \right] \times \sqrt{2\pi} \left[|\omega.F.T.\{f(t)\}|_{\omega=\omega_p}^2 \right]^{1/2} \sin[\omega_p t + \arg[F.T.\{f(t)\}]] \quad (9),$$

where F.T. indicates a Fourier transformation. The maximum wakefield amplitude for a given pulse shape can thus be found by simply evaluating the Fourier transformation of the longitudinal pulse shape function at ω_p . The optimum pulse width of a few pulse shapes for maximum wakefield amplitude generation is shown in Table 1.

Expressing the scaling law for the resonant density in terms of laser pulse width τ we obtain

$$n_0 [\text{cm}^{-3}] = \frac{\kappa^2 \cdot 3.1 \times 10^{21}}{\tau^2 [\text{fs}]} \quad (10),$$

where the plasma density and pulse width are in units of cm^{-3} and femtoseconds respectively. The resonant density for a 50 fs long Gaussian pulse is about $7 \times 10^{17} \text{ cm}^{-3}$.

$I(s)$	$\sigma(\text{FWHM})$	$\kappa; \omega_p \tau = \kappa \pi$
e^{-2s^2}	$\sqrt{2 \ln 2} \approx 1.386$	$\frac{2}{\pi} \sqrt{2 \ln 2} \approx 0.75$
$\Pi(s) = \begin{cases} 1 & s < \frac{1}{2} \\ 0 & s > \frac{1}{2} \end{cases}$	1	1
$\text{sech}(\pi s)$	0.84	0.64
$\Pi(s) \cos(\pi s)$	2/3	0.9115
$\frac{\sin^2(\pi s)}{\pi^2 s^2}$	0.8859	0.8859

Table 1: Scaling factor κ , where $\kappa = \frac{\omega_p \tau}{\pi}$, and normalized pulse width $\sigma(\text{FWHM})$ for various longitudinal laser pulse shapes $I(s)$ where s represents unit-less time.

The plasma wavelength λ_p corresponding to the resonant plasma density can be written as

$$\lambda_p [\mu\text{m}] = 0.6 \frac{\tau [\text{fs}]}{\kappa} \quad (11)$$

which gives 40 μm for the example. Also, the ratio of collisionless kin depth to spot size is then $k_p r_0 = 2.67$ and 6.7 for Case A and B respectively. To guide the laser pulse the parabolic channel requires a depth $\Delta n_r = (\pi r_0^2)^{-1}$ of 3.91×10^{17} (6.4×10^{16}) cm^{-3} for

Case A (B) respectively. The relativistic group velocity factor $\gamma_g = (1 - \beta_g^2)^{-1/2}$ for underdense plasmas is given by $\gamma_g \approx \frac{\omega}{\omega_p} = \frac{\lambda_p}{\lambda_0}$ or, in terms of laser parameters,

$$\gamma_g = 0.6 \frac{\tau[\text{fs}]}{\kappa \cdot \lambda_0[\mu\text{m}]} \quad (12)$$

For the numerical example we then have $\gamma_g = 50$. The normalized quiver momentum of an electron in the field of the driving laser can be written as

$$a_0 \equiv 4.8 \lambda_0[\mu\text{m}] \sqrt{\frac{P[\text{TW}]}{(r_s[\mu\text{m}])^2}} \quad (13)$$

which gives a_0 equal to 0.72 (0.286) for Case A (B). The maximum on-axis longitudinal electric field strength in the one-dimensional limit is given by [18]

$$E_{\text{max}}[\text{GeV}/\text{m}] \equiv 3.8 \times 10^{-8} (n_0[\text{cm}^{-3}])^{1/2} \frac{a_0^2}{\sqrt{1 + \frac{a_0^2}{2}}} \quad (14).$$

Rewriting E_{max} in terms of laser parameters we find

$$E_{\text{max}}[\text{GeV}/\text{m}] \equiv 9.74 \times 10^4 \left(\frac{\lambda_0}{r_s} \right)^2 \frac{\kappa P[\text{TW}]}{\tau[\text{fs}]} \quad (15).$$

Here it is assumed that a_0^2 and the $\delta n/n_0$ are both much less than one. Numerically E_{max} is then 15.9 (2.6) GeV/m for Case A (B).

In the absence of laser guiding, the accelerating distance will be limited to the diffraction length $L_{\text{diff}} = \pi Z_R = \frac{\pi^2 r_s^2}{\lambda}$. The maximum energy gain of a test particle is then given by

$$\Delta W_{\text{diff}}[\text{MeV}] = 960 \frac{\kappa \lambda_0[\mu\text{m}]}{\tau[\text{fs}]} P[\text{TW}] \quad (16)$$

which is independent of laser spot size. Using Eqn. (11) we can rewrite Eqn. (16) as

$$\Delta W_{\text{diff}} [\text{MeV}] \cong 576 \frac{\lambda_o [\mu\text{m}]}{\lambda_p [\mu\text{m}]} P [\text{TW}] \quad (17)$$

which gives $\Delta W_{\text{diff}} = 57.6 \text{ MeV}$ for the example.

Assuming that diffraction of the laser pulse can be overcome inside a parabolic channel, the maximum distance of acceleration becomes the lesser of the dephasing length $L_{\text{deph}} = \gamma_g^2 \lambda_p = \frac{\lambda_p^3}{\lambda_o^2}$ or the pump depletion length $L_{\text{pump}} = \frac{L_{\text{deph}}}{a_o^2}$. In the small a_o limit, which we have assumed throughout this design study, the acceleration distance will be taken to be the dephasing length since it is always shorter than the pump depletion length. Rewriting L_{deph} in terms of laser parameters we obtain

$$L_{\text{deph}} \cong 2.16 \times 10^{-7} \frac{\tau^3 [\text{fs}]}{\kappa^3 (\lambda_o [\mu\text{m}])^2} \quad (18)$$

The maximum energy gain after a dephasing distance is then given by

$$\Delta W_{\text{ch}} [\text{MeV}] \cong 2.1 \times 10^{-2} \frac{\tau^2 [\text{fs}]}{\kappa^2 r_s^2 [\mu\text{m}]} P [\text{TW}] \quad (19)$$

or, alternatively,

$$\Delta W_{\text{ch}} [\text{MeV}] \cong 60 \left(\frac{\lambda_p}{r_s^2} \right)^2 P [\text{TW}] \cong 2.4 \times 10^3 \frac{P [\text{TW}]}{(k_p r_s^2)^2} \quad (20)$$

We then find $\Delta W_{\text{ch}} \cong 1.7 \text{ GeV}$ for Case A and 266 MeV for Case B. If we include 3D effects, the maximum energy gain on axis is increased by the factor $1 + 8/(k_p r_s^2)^2$, in accordance with Eqns. (7-9), which for Case A (B) is 2.13 (1.18). The design results are summarized in Table 2.

	Case A	Case B
Laser Power P[TW]	5	5
Laser pulse length τ [fs]	50	50
Resonant plasma density [cm^{-3}]	7×10^{17}	7×10^{17}
Beam radius, r_s [μm]	17	42
$k_p r_s$	2.7	6.7
Plasma density at $r = r_s$	1.09×10^{18}	7.64×10^{17}
Laser strength, a_0	0.72	0.29
Rayleigh length, Z_R [mm]	1.13	7.07
Dephasing length [mm]	100	100
Accelerating gradient, E_z [GeV/m]	16.2	2.6
Max. energy gain no guiding, ΔW_{diff} [GeV]	0.057	0.057
Maximum energy gain with guiding, ΔW_{ch} [GeV]	1.7	0.26

Table 2: Summary of design parameters for second generation guiding and wakenfield excitation experiments. The design was carried out using 1D design equations. Including 3D effects, the maximum energy gain on axis could be a factor 2.13 (1.18) larger in Case A (B).

As discussed before, to minimize the effect radial electric fields have on beam emittance, the particle beam size should be small compared to the scale length of the transverse uniformity of the excited wakefields. Detailed simulations of the excitation of wakefields in the parabolic channel and coupling of an electron beam into the structure will be the subject of future work.

A more global overview of the parameter regimes relevant for second generation experiments can be obtained from Figs. 1, 2 and 3. From the previous discussion it is apparent that, for a given laser wavelength and laser spot size, the two key laser system characteristics which parametrize the design are the laser pulse length τ and energy W_p (respectively the x and y-axis in the Figures). From Eqns. (12), (10) and (18) respectively we find that for a Gaussian laser pulse $\gamma_g = \tau[\text{fs}]$, that the resonant density is proportional to τ^{-2} and that the dephasing length is proportional τ^3 . These dependencies are shown on the additional horizontal axis. Limitations on the average power and on damage fluence (typically $< 2 \text{ J/cm}^2$) of the present laser systems allow us to put a repetition rate and a required final amplifier diameter axis (vertically). Constant laser power lines are shown as dashed lines. In Figure 1, we have shaded an area where table top GeV accelerators most likely will operate: $E_z > 1 \text{ GeV/m}$ (allows for a compact accelerator) and where $P < P_{\text{crit}}$ (avoids being in a highly non-linear regime). In Figure 2, iso-energy gain lines are shown for the case where the acceleration distance is limited to the diffraction length. In Fig. 3 iso-energy gain lines are shown for the case with guiding over the lesser of the dephasing or pump-depletion length.

IV. SIMULATION OF CASES A AND B DESIGNS

To validate some of the scaling law results, we have carried out numerical simulations of the wakefield excitation by short laser pulses in parabolic channels for the cases A and B. The simulation used a weak non-linear model for the laser field amplitude and plasma density perturbations (with a prescribed radial dependency of $\omega_p(r)$ in the channel) [22-24]. The parameters for case B were chosen in full agreement with Table 2. For case A it was necessary to reduce the depth of the channel ($n(r = r_s) = (7+2.1) \times 10^{17}$), from its value theoretical prediction indicated in the Table. For deeper channels, higher order transverse modes were excited and the structure of the wakefield was found to be inappropriate for particle acceleration.

The normalized amplitude of density perturbations in the wake ($\delta n / n_0$) (upper plots) and the maximum of the laser field amplitude (a_0) (lower plots) on the plasma channel axis ($r=0$) are plotted as function of the normalized laser pulse propagation length z / Z_R for the cases A and B (left and right plots) in Fig.4.

The laser field amplitude and the plasma wake exhibit an oscillatory behavior while propagating along the channel. In case B, for which the plasma wake amplitude is relatively small, these pulsations are mainly due to the difference of the power in different cross sections of the laser pulse [24]. They cannot be avoided as the relativistic nonlinearity does not allow a full adjustment of the channel for all cross sections of the pulse (see Eq.(3)). As is seen in Fig. 4, the effect is much more pronounced for a smaller beam radius (case A), i.e. higher laser intensities and plasma wave. It should be noted that, since the parameters for case A are on the upper boundary of the model's applicability ($k_p r_s > 1$, $a_0^2 < 1$, $\delta n / n_0 < 1$), the results are believed to be only qualitatively correct. The comparison of the simulation results for the cases A and B clearly shows however, that for the purposes of particle acceleration, the laser pulse radius should be chosen between the cases A and B.

At the same time, the plasma wave amplitude is then large and the oscillations of the wake amplitude, while propagating along the channel, remain small enough.

V. EXPERIMENTAL ISSUES

A. Plasma Production

The guiding and wakefield excitation experiments will require development of plasma channels in a controllable and reproducible way. The most successful technique thus far of channel production has been to rely on hydrodynamic expansion of a laser produced and heated plasma in a gas filled vacuum chamber. [10] Long plasmas with a small transverse size have been created by focusing a relatively long (100 ps) energetic (1 J) laser pulse to a line focus with an axicon lens. Although experiments have shown guiding of 100 ps long laser pulses with intensities up to 5×10^{14} W/cm², direct measurement of the plasma profile has not been carried out yet. From hydrodynamic simulations it was concluded that typical plasma densities on axis are on the order of 10^{19} cm⁻³ with a typical channel width on the order of 10 μ m. Since both the laser propagation and wakefield generation are strongly dependent on the properties of the channel, future experiments should attempt a full characterization of the plasma.

Guiding of an intense, ultrashort laser pulse in a rare gas plasma can potentially also be accomplished in a cylindrical wave guide in which a guiding refractive index profile is produced by an acoustic standing wave pattern. Using a thin walled piezoelectric tube excited for radial vibration at frequency ω_{ac} , a standing wave neutral density gas perturbation $\delta\rho$ can be established such that $\delta\rho \propto J_0(\omega_{ac}r/c_s)\cos\omega t$, where c_s is the sound speed of the gas and J_0 is the zeroth order Bessel function. Near $r = 0$, the Bessel function has the required parabolic radial dependence necessary to guide a Gaussian shaped laser pulse. The acoustic resonance frequency ω_{ac} is chosen so that the difference in the refractive index at $r = 0$ and $r = r_s = 2.4 c_s / \omega_{ac}$ is sufficient to guide a laser pulse with a spatial profile given by $I = I_0 \exp(-2r^2/r_s^2)$. For example, to guide a laser pulse with a spot size of $r_s = 17 \mu$ m (42 μ m) in He ($c_s \approx 1000$ m/s), the resonant frequency is $\omega_{ac} = 141$

MHz (57 MHz). During one half cycle of the acoustic standing wave, the neutral gas density will be minimum on axis, and once ionized by an intense laser pulse, a radial electron density profile will be created with an electron density minimum on axis [10]. It should be mentioned that during the other half cycle of the standing wave, the neutral gas density on axis will be at a maximum and can guide a laser pulse that does not ionize the gas.

Although simple in concept, a number of problems must be overcome in order for the piezo-tube to be a viable guiding mechanism. Since the resonance frequency of a tube with a wall thickness d scales as $f_r \approx 1000/d(\text{m})$, the tube must have a wall thickness less than 1 mm in order to reach MHz resonant frequencies. Such thin walled tubes have high capacitance and large power dissipation. Therefore, the piezo tube must be cooled so that its temperature remains well below the Curie temperature ($T_c \approx 300^\circ\text{C}$), the temperature at which the ceramic loses its piezoelectric properties. In order to excite a single mode standing wave, the inside radius of the piezo tube must be formed with a radial tolerance of less than the spot size of the laser. The absorption of sound waves in the gas is also of importance at high frequencies. In 1 atm He at $\omega_{ac}/2\pi = 10\text{MHz}$, the classical absorption coefficient is 5.3 cm^{-1} [25]. Consequently, the piezo must be driven with larger displacements in order to achieve the guiding standing wave pattern. Finally, since ionization does not occur on the leading edge of the laser pulse, the leading edge of the laser pulse will not be guided by the refractive index profile that favors guiding in the plasma.

B. Diagnostics for Guided Laser Wakefield Structures

In addition to plasma channel density profile characterization, second generation experiments will require sophisticated optical and particle beam based diagnostics for wakefields. A complete discussion of optical diagnostics can be found in the article by

Siders et al. [26] Briefly summarizing their results, an optical witness pulse sent with an appropriate delay behind the driver pulse will experience a red/blue-shifting [27-28] depending on whether the witness pulse sees a lower or higher density than the ambient plasma density. The amount of phase $\Delta\phi / \pi$ and frequency shifting $\Delta\omega / \omega$ for resonant wakefield excitation is approximately given by

$$\begin{aligned}\frac{\Delta\phi}{\pi} &\approx 10^5 \left(\frac{\lambda}{\tau}\right)^3 \left(\frac{L}{A}\right) W_p \\ \frac{\Delta\omega}{\omega} &\approx 10^5 \left(\frac{\lambda}{\tau}\right)^4 \left(\frac{L}{A}\right) W_p\end{aligned}\tag{21}$$

where W_p is the laser pulse energy in Joules; τ is the pulse width in femtoseconds; λ , L , A , are the laser wavelength, interaction length, and cross-sectional area in μm and μm^2 . We can see from these equations that the most significant route to large signal is to use the shortest τ as practical. Clearly changes in pulse energy have a linear advantage. In the case of a Gaussian focus, the factor L/A is independent of focal length and hence no advantage may be gained by altering the focal geometry. With optical guiding, though, this factor may provide an additional one to two orders of magnitude in signal. For example, an upper limit on L/A may be placed by assuming that L corresponds to the dephasing length, while $A \propto \pi\lambda_p^2$. For this upper limit case,

$$\begin{aligned}\frac{\Delta\phi}{\pi} &\approx 0.25 \times 10^5 \left(\frac{\lambda}{\tau^2}\right) \left(\frac{L}{A}\right) W_p \\ \frac{\Delta\omega}{\omega} &\approx 0.25 \times 10^5 \left(\frac{\lambda^2}{\tau^3}\right)^4 \left(\frac{L}{A}\right) W_p\end{aligned}\tag{22}$$

which give $\Delta\phi \geq \pi$ and $\Delta\omega / \omega \geq 10^{-1}$. As the laser bandwidth is typically about $10^{-2} \omega$ this represents an obviously significant magnitude shift.

Particle beam based diagnostics will allow direct measurement of the longitudinal and radial fields generated in the plasma channel. Wakefield measurements utilizing injectors with pulses long compared to the plasma period will be complicated to interpret,

due to the fact that electrons will be injected at all phases into the wake. Development of beam diagnostics with femtosecond time and micron spatial resolution seem essential for those experiments. Of course, synchronization requirements will not be severe. As was discussed before, detailed simulations of the excitation of wakefields in a parabolic channel and coupling of an electron beam into such a structure will be required to determine the requirements of the particle injector. More detailed discussions on the injector requirements for a second generation experiment can be found in the article by Serafini et al..[29]

VI. PLASMA WAVE EFFECTS ON OPTICALLY GUIDED LASER PULSES

The scaling laws, which were used in Section III for the design of a second generation guiding and wakefield excitation experiment, did not include self-consistent effects between the laser beam and the plasma and ignored the effect of instabilities. The choice of pulse length (essentially half the plasma period) validates ignoring instabilities with long growth times. However, as will be discussed, transverse and longitudinal effects can develop, while the pulse propagates through the channel and excites plasma wakes, which can result in important changes in group velocity of the laser pulse and phase velocity of the plasma wake, as well as in transverse mode structure changes and whole-beam displacement through laser hosing. [9, 30-31]

To lowest order, the acceleration distance in a laser-plasma accelerator is the smallest of the diffraction, the dephasing and the pump depletion length. In this article the use of a preformed density channel is considered to overcome diffraction. For the parameters we will consider, the pump depletion length is longer than the dephasing length. However, as the drive pulse propagates down the channel its shape distorts due to the wake that it is generating. This distortion can be due to transverse and longitudinal bunching of the laser energy. As the pulse distorts the wake left behind changes and although these changes are relatively minor they can change the effective phase velocity of the wake. Since the dephasing length is a very sensitive function of v_p , pulse distortion could limit the acceleration distance to a distance shorter than the dephasing distance L_d , where $L_d = (\omega^2 / \omega_p^2) \lambda_p$.

A. Externally generated plasma wave

We first consider effects of an externally generated plasma wave on the focusing/diffraction of a 'test' laser pulse. We will assume that the test laser pulse does not

affect the externally generated plasma wave and does not generate a plasma wave (wakefield) of its own. The test laser pulse is assumed to propagate in a parabolic density channel of the form $\Delta n_p = \Delta n r^2 / r_0^2$ in the presence of a plasma wave of the form $\delta n = \delta n_0 \sin k_p \zeta \exp(-r^2 / r_p^2)$, i.e., a Gaussian radial profile with a radius r_p and a phase velocity $v_p \cong c$. The equation describing the evolution of the laser spot size r_s has been given in Section II, Eqn. (3).

Consider the effects of a plasma wave on a long ($L \gg \lambda_p = 2\pi c / \omega_p$, L = pulse length) axially uniform, matched pulse [15] i.e., a pulse for which $P / P_c = 1 - \Delta n / \Delta n_c$. Equation (3) indicates that for $\delta n_0 > 0$, the plasma wave produces periodic regions of enhanced focusing (where $\sin k_p \zeta < 0$) and enhanced diffraction (where $\sin k_p \zeta > 0$). Here, $\zeta \leq 0$ can be taken as a measure of the distance back from the head $\zeta = 0$ of the laser pulse (the laser pulse exists in the region $-L \leq \zeta \leq 0$). Hence, the initial effects of the plasma wave will be to modulate an initially uniform pulse into periodic segments which are centered about the regions of strongest focusing ($\sin k_p \zeta = -1$ for the present example). Notice that the intensity tends to modulate such that the intensity peaks correspond to the density minima of the plasma wave. In other words, for small modulations, the intensity modulation is 180° out of phase with the density modulation. This is illustrated schematically in Fig. 5.

The spot size evolution can be estimated from Eqn.(3) by expanding about the matched beam conditions $R = 1 + \delta R$ and $P / P_c = 1 - \Delta n / \Delta n_c$, and by treating the plasma wave as a perturbation. Initially, for $z < Z_R$ the spot size evolves according to

$$\delta R \cong (z / Z_R)^2 (\delta n_0 / 4 \Delta n_c) \sin k_p \zeta \quad (23).$$

assuming $r_p^2 \cong r_0^2 / 2$. The regions of strongest focusing occur at $\sin k_p \zeta = -1$. Notice that the strength of the plasma wave focusing depends on the plasma wave amplitude relative to the critical channel depth, $\delta n_0 / \Delta n_c = (k_p^2 r_0^2 / 4) \delta n_0 / n_0$.

B. Self-consistent plasma wave

The above discussion neglected the effect of the laser pulse on the plasma wave and described how an external plasma wave would modulate an initially uniform, low-intensity laser pulse. In laser-driven accelerator schemes, however, it is the laser pulse structure which produces the plasma wave and the laser pulse evolution must be examined self-consistently. Consider, for example, a plasma wave generated by a fully modulated laser pulse with an axial profile of the form $f(\zeta) = 1 - \cos k_p \zeta$, for $-L < \zeta < 0$, as in the PBWA. This will resonantly drive a plasma wave of the form [20]

$$\delta n / n_0 \equiv (a_0^2 / 4) k_p \zeta \sin k_p \zeta \quad (24)$$

Notice that the plasma wave is secularly growing behind the head of the laser pulse $\zeta < 0$. Furthermore, the plasma wave and laser pulse are 90° out of phase. For a laser pulse structure which is being guided, as discussed in the previous section, the plasma wave will tend to produce intensity modulations which are 180° out of phase with the density wave. For the self-consistent case, however, $a^2 \propto 1 - \cos k_p \zeta$ and $\delta n / n_0 \propto -\sin k_p \zeta$. The intensity maxima lie on the maximum gradients in the density wave. Consider a single intensity peak located at $k_p \zeta = -\pi$. The back portion of the peak in the region $-2\pi < k_p \zeta < -\pi$ will see a local density channel which provides enhanced focusing. The front portion of the peak in the region $-\pi < k_p \zeta < 0$ will experience enhanced diffraction. This will cause the intensity peaks to deform, the front diffracting and the back focusing. In effect, this deformation causes the intensity peak to shift backward (towards the density minima) with respect to the plasma wave.[32] As the evolving laser pulse structure continues to drive the plasma wave, a subsequent effect of the backward shifting of the intensity peaks is a reduction in the effective phase velocity of the plasma wave.[32]

An envelope equation for the evolution of the spot size r_s , including the self-consistent density response given by Eqn.(4), has been derived in Ref. [17]. For $z < Z_R$

and $k_p^2 \zeta^2 \gg 1$ (sufficiently far behind the front of the laser pulse), this envelope equation reduces to Eqn. (3) with $r_p^2 = r_s^2 / 2$ and with $\delta n_0 \sin k_p \zeta$ replaced by the value of δn given by Eqn. (24). Perturbing about the matched beam solution, $R = 1 + \delta R$, with $\delta R^2 \ll 1$, the initial evolution of the spot size is found to be given by Eqn. (23) with $\delta n_0 \sin k_p \zeta$ replaced by the value of δn given by Eqn. (24). Hence, $\delta R = \delta R_0(z) \sin k_p \zeta$, where $\delta R_0 = -(z^2 / Z_R^2)(\delta n_0 / 4\Delta n_c)$ and $\delta n_0 / n_0 = -(a_0^2 / 4)k_p \zeta$ is the amplitude of the beat-generated plasma wave.

The laser intensity along the $r = 0$ axis is given by $I = I_0 r_{so}^2 / r_s^2$, where I_0 is the initial axial intensity profile. Within the paraxial approximation, the laser power $P \propto I r_s^2 = I_0 r_0^2$ is constant (independent of z). As the laser spot size evolves, the intensity on axis changes. For small changes in the spot size $r_s = r_0 + \delta r_s(z, \zeta)$, $I \cong I_0 [1 - 2\delta R(z, \zeta)]$, where $\delta R = \delta r_s / r_0$. Consider a laser beat wave with an initial intensity on axis of $I_0 = (I_p / 2)(1 - \cos k_p \zeta)$, where I_p is the peak intensity. As discussed in the preceding paragraph, the spot size perturbation is given by $\delta R = \delta R_0(z) \sin k_p \zeta$. Hence, the initial evolution of the intensity on axis is given by

$$I \cong (I_p / 2)(1 - \cos k_p \zeta) [1 - 2\delta R_0(z) \sin k_p \zeta] \quad (25)$$

This indicates that the intensity maxima occur at the phase positions $k_p \zeta \cong k_p \zeta_0 + 4\delta R_0$, where $\zeta_0 = -(2l + 1)\pi / k_p$ ($l = \text{integer}$) are the initial ζ positions of the maxima. This implies that the effective group velocity [14] $v_g = c\beta_g$ of the intensity maxima is $\beta_g \cong \beta_{g0} + (4 / k_p) \partial(\delta R_0) / \partial z$, where $v_{g0} = c\beta_{g0}$ is the group velocity in

the absence of the plasma wave. In terms of the amplitude of the density wave,

$$\Delta\beta_g = -(z / Z_R)(k_p / k)(\delta n_0 / n_0) \quad (26)$$

where $\Delta\beta_g = \beta_g - \beta_{g0}$ and $\lambda = 2\pi / k$ is the laser wavelength. In the 1D limit, $\beta_{g0} = 1 - k_p^2 / 2k^2$, assuming $k_p / k \ll 1$. Hence, the reduction in the group velocity

becomes significant when $(z/Z_R)(\delta n_o/n_o) > k_p/k$. Since the intensity modulations drive the plasma wave, the plasma wave phase velocity is reduced by approximately $\Delta\beta_p \equiv \Delta\beta_g$.

This general behavior is observable in pulses undergoing self-modulation.[17,32] To illustrate this, the envelope equation for the laser spot size given in Ref.[17] is solved numerically for a flattop laser pulse.[32] The initial axial intensity profile is chosen to consist of a ramp up region in which a^2 rises from zero at $\zeta = 0$ to a value of $a_0 = 0.028$ at $\zeta = -5\lambda_p$, followed by a long flattop region with $a_0 = 0.028$ for $\zeta < -5\lambda_p$. The flattop region of the pulse is primarily channel guided with $\Delta n / \Delta n_c = 0.9$, $P/P_c = 0.1$, $n_0 = 1.24 \times 10^{16} \text{ cm}^{-3}$ ($\lambda_p = 300 \mu\text{m}$), $r_0 = 0.3 \text{ cm}$, and $\lambda = 1 \mu\text{m}$. As the pulse propagates, it begins to self-modulate. The normalized intensity modulation $\delta a^2 / a_0^2$ (dashed line), where $\delta a^2 = a^2 - a_0^2$, and the normalized plasma density wave $\delta n / n_0$ (solid line), are plotted as a function of ζ / λ_p after propagating a distance $z = 6.4 Z_R$ in Fig. 6(a) and $z = 8.0 Z_R$ in Fig. 6(b). Clearly the modulations are growing from the front of the pulse backward and as a function of z . Notice that the intensity and density modulations are approximately 90° out of phase and are phased such that the front a particular intensity modulation sees an increase in density and the back sees a locally enhanced channel. In particular, notice how a particular intensity peak in Fig. 6(a) has slipped backward in ζ in Fig. 6(b). This relative backward motion of the intensity peaks is due to a reduction in the effective group velocity $\Delta\beta_g < 0$, as discussed in the previous paragraphs.

Another example of a transverse instability is the so called laser-hosing instability.[9,30] When self-consistent interaction between the laser pump and the wake are taken into account, one finds that very small distortions of the transverse profile of the laser pulse can exponentially amplify after a number of Rayleigh lengths [9,30]. The physics of this instability is rather straightforward: a small transverse distortion near the head of the laser pulse leaves a plasma wake of the same transverse shape behind which then acts on

the tail of the pulse leading to an even larger distortion. Various regimes of this instability, corresponding to different pulse lengths and propagation distances, were studied in Ref.[9].

C. Longitudinal Plasma Wake Effects

We now estimate the amount of pulse distortion expected from longitudinal effects within the zeroth order dephasing distance. Consider a short pulse of length $c\tau_p = L \approx \lambda_p / 2$. To zeroth order the front of the pulse resides in a density compression while the back of the pulse resides in a density rarefaction. Therefore, the front and back move at different group velocities (v_{gf} and v_{gb} respectively) with the back moving forward with respect to the front. This leads to a change in the pulse length of

$$\begin{aligned} \Delta c\tau_p &= (v_{gf} - v_{gb})\Delta ct \\ &\equiv -\frac{\omega_p^2}{\omega^2} \frac{\delta n}{n_0} \Delta ct \end{aligned} \quad (27)$$

Since the wakefield generation by a short laser pulse is a nonresonant process, we can assume that the laser action W_p/ω is conserved. Physically this corresponds to the red-shifting of the laser as it loses energy to the plasma wave. This can be expressed as

$$a_0^2 (c\tau_p)^2 = \text{constant} \quad (28),$$

and the decrease in the pulse length implies an increase in the pulse intensity, i.e.,

$$\Delta a_0^2 (c\tau_p)^2 + 2a_0^2 (c\tau_p) \Delta c\tau_p = 0 \quad (29)$$

or

$$\Delta a_0^2 = -2a_0^2 \frac{\Delta c\tau_p}{c\tau_p} \quad (30)$$

Therefore,

$$\frac{\Delta a_0^2}{a_0^2} = 2 \frac{\omega_p^2}{\omega^2} \frac{\delta n}{n_0} \frac{\Delta ct}{c\tau_p} \quad (31)$$

and if we assume $c\tau_p = \lambda_p / 2$, then we obtain for the amount of distortion within a dephasing length $\Delta ct = (\omega^2 / \omega_p^2) \lambda_p$

$$\frac{\Delta a_0^2}{a_0^2} = 4 \frac{\delta n}{n} \quad (32).$$

The result is independent of ω_p^2 / ω^2 and generally near unity, so longitudinal pulse distortion needs to be considered for any laser wakefield experiment in which the interaction distance approaches the dephasing distance.

To see this further, we estimate the change in δn of the wake by using the spatial-temporal gain formula for Raman forward scattering [32]

$$G = I_0 \left(\frac{a_0}{\sqrt{2}} \frac{\omega_p}{\omega} \sqrt{t\tau_p \omega_p^2} \right) \quad (33)$$

where I_0 is the zeroth order modified Bessel function of the first kind. The change in the wake's amplitude during a dephasing distance is given by $\delta n = \delta n_0 G$ where δn_0 is the initial wake amplitude. Assuming $\omega_p \tau_p = \pi$ and $\omega_p t = 2\pi \omega_p^2 / \omega^2$ gives

$$\delta n = \delta n_0 I_0(\pi a_0) \quad (34)$$

which for $a_0 \cong 1$ predicts that δn will increase by a factor of five. Clearly, longitudinal pulse distortion and its effect on the wake needs to be considered. Last, we note that the wake's phase velocity will depend on the initial pulse shape.[34] This is also an area of future work.

VII. CONCLUSION

A design study has been carried out for a second generation experiment on laser guiding and wakefield excitation in a channel. To emphasize the laser driver requirements we have expressed simple scaling laws for the wakefield amplitude, dephasing length, γ_g and energy gain with and without guiding, in terms of laser pulse length, wavelength, power and spot size. This has allowed us to define an optimum parameter regime for the laser systems capable of driving a plasma based accelerator structure, which could be used as a compact single stage GeV accelerator and/or as a single-stage component of larger systems. We find that the parameter regime favors laser systems producing short pulses ($10\text{fs} \leq \tau \leq 100\text{fs}$), each containing an energy on the order of 100 mJ to a few J's. With current day technology such systems operate at a repetition rate of 1 Hz for the high energy/pulse case and at the 1 kHz rate for the lower energy/pulse case. Taking the dephasing length as the maximum acceleration distance, plasma channels with lengths of 1 mm to 10 cm and densities of 10^{17} cm^{-3} up to 10^{19} cm^{-3} need to be produced.

Although in principal a hollow channel has superior accelerating properties, production of parabolic channels seems at the present experimentally more accessible. Plasma production techniques will need to be developed for accelerator applications, which allow full control of the transverse and longitudinal channel profiles and lead to optimal and extremely reproducible channel properties. Some issues associated with the production of channels by means of a piezo-electric driven cylinder were discussed.

Plasma profile diagnostics and wakefield diagnostics will need to be developed for channel experiments. We briefly discussed optical as well as particle based wakefield diagnostics. A simple engineering scaling law was given for the phase and frequency shift that a witness optical pulse sees when it propagates in the plasma wake of a high intensity laser pulse. Wakefield measurement with particle beams will require the development of

high resolution temporally and spatially resolved beam diagnostics. Ideally, ultra-short (10 fs) low emittance injectors, which are synchronized to the drive laser, will be required.

The design studies presented in this paper have been primarily concerned with the most basic physics issues of a LWFA: diffraction and channel guiding, dephasing and depletion limits, and linear wakefield theory. Other issues, such as laser-plasma instabilities, laser pulse distortion, and wakefield damping, deserve continued theoretical and self-consistent computational investigation. Several aspects of the effect of the plasma wave on the evolution of the laser pulse were discussed in Sec. VI. These transverse and longitudinal pulse distortions deleteriously affect the generated plasma wave phase velocity and amplitude, and hence may limit the achievable energy gains over the 1D linear estimates. Finally, the laser-hose instability, by causing channel deformation along the direction of propagation, could provide a nonlinear contribution to the emittance of injected particle bunches. These issues are currently under investigation.

Although many nonlinear effects have been predicted, with the present technology, meaningful experiments are possible in which prototype small accelerators (100 MeV - 1 GeV, cm scale) can be developed which will serve to evaluate the future of laser plasma accelerator.

VIII. ACKNOWLEDGMENTS

One of the authors (E.E.) acknowledges useful conversations with J. Krall and P. Sprangle. This work was supported by the Department of Energy and the Office of Naval Research.

References

- [1] T. Tajima and J.M. Dawson, "Laser electron accelerator", *Phys. Rev. Lett.*, vol. 43, 267 (1979); "Advanced Accelerator Concepts", edited by P. Schoessow, *AIP Conf. Proc.* vol. 335, 1995; E. Esarey, P. Sprangle, J. Krall, and A. Ting, "Overview of plasma-based accelerator concepts", this issue.
- [2] L. M. Gorbunov and V.I. Kirsanov, *Sov. Phys. JETP*, vol. 66, p. 290, 1987; P. Sprangle, E. Esarey, A. Ting and G. Joyce, "Laser wakefield acceleration and relativistic optical guiding", *Appl. Phys. Lett.*, vol. 53, pp. 2146-2148, 1988; E. Esarey, A. Ting, P. Sprangle, and G. Joyce, "The laser wakefield accelerator", *Comments Plasma Phys. Controlled Fusion*, vol. 12, pp. 191-204, 1989.
- [3] D. Umstadter, E. Esarey, and J. Kim, "Nonlinear plasma waves resonantly driven by optimized laser pulse trains", *Phys. Rev. Lett.*, vol. 72, pp. 1224-1227, 1994.
- [4] C. E. Clayton, K. A. Marsh, A. Dyson, M. Everett, A. Lal, W. P. Leemans, R. Williams, and C. Joshi, "Ultra-high-Gradient Acceleration of Injected Electrons by Laser-Excited Relativistic Electron Plasma Waves", *Phys. Rev. Lett.*, vol. 70, pp. 37 - 40, 1993; F. Amiranoff et al., "Electron acceleration in Nd-laser plasma beat-wave experiments", *Phys. Rev. Lett.*, vol. 74, pp. 5220-5223, 1995.
- [5] Nakajima et al., "Observation of ultrahigh gradient electron acceleration by a self-modulated intense short laser pulse", *Phys. Rev. Lett.*, vol. 74, pp. 4428-4431, 1995.
- [6] T. Tajima, "High energy laser plasma accelerators", *Laser and Part. Beams*, vol. 3, pp. 351-413;

- [7] P. Sprangle, E. Esarey, J. Krall, and G. Joyce, "Propagation and guiding of intense laser pulses in plasmas", *Phys. Rev. Lett.*, vol. 69, pp. 2200, 1992; E. Esarey, P. Sprangle, J. Krall, A. Ting and G. Joyce, "Optically guided laser wakefield acceleration", *Phys. Fluids B*, vol. 5, pp. 2690-2697, 1993.
- [8] T. C. Chiou, T. Katsouleas, C. Decker, W.B. Mori, G. Shvets, and J.S. Wurtele, "Laser wake-field acceleration and optical guiding in a hollow plasma channel", *Phys. Plasmas*, vol. 2, pp. 310-318, 1995.
- [9] G. Shvets and J. S. Wurtele, "Instabilities of short-pulse laser propagation through plasmas", *Phys. Rev. Lett.*, vol. 73, pp. 3540, 1994; G. Shvets, "Interaction of intense lasers with plasmas", Ph.D. dissertation, MIT, 1995, unpublished.
- [10] C.G. Durfee III and H. M. Milchberg, "Light pipe for high intensity laser pulses", *Phys. Rev. Lett.*, vol. 71, pp. 2409, 1993; C.G. Durfee III, J. Lynch, and H.M. Milchberg, "Development of a plasma wave guide for high intensity laser pulses", *Phys. Rev. E*, vol. 51, pp. 2368, 1995.
- [11] C. Max, J. Arons and A.B. Langdon, "Self-modulation and self-focusing of electromagnetic waves in plasmas," *Phys. Rev. Lett.*, vol. 33, pp. 209-212, 1974.
- [12] P. Sprangle, C.M. Tang, and E. Esarey, "Relativistic self-focusing of short-pulse radiation beams in plasmas," *IEEE Trans. Plasma Sci.*, vol. PS-15, pp. 145-153, 1987.
- [13] G.Z. Sun, E. Ott, Y.C. Lee, and P. Guzdar, "Self-focusing of short intense pulses in plasmas," *Phys. Fluids*, vol. 30, pp. 526-532, 1987.
- [14] W.B. Mori, C. Joshi, J.M. Dawson, D.W. Forslund, and J.M. Kindel, "Evolution of self-focusing of intense electromagnetic waves in plasma," *Phys. Rev. Lett.*, vol. 60, pp. 1298-1301, 1988.

- [15] E. Esarey, A. Ting, and P. Sprangle, "Optical guiding and beat wave phase velocity control in the plasma beat wave accelerator", in *Advanced Accelerator Concepts*, edited by C. Joshi, AIP Conf. Proc. vol. 193 , pp. 71-86, 1989.
- [16] P. Sprangle, E. Esarey, and A. Ting, "Nonlinear theory of intense laser-plasma interactions," *Phys. Rev. Lett.*, vol. 64, pp. 2011-2014, 1990; "Nonlinear interaction of intense laser pulses in plasmas," *Phys. Rev. A*, vol. 41, pp. 4463-4469, 1990.
- [17] E. Esarey, J. Krall, and P. Sprangle, "Envelope analysis of intense laser pulse self-modulation in plasmas", *Phys. Rev. Lett.*, vol. 72, pp. 2887-2890, 1994.
- [18] G. Shvets and J. S. Wurtele, "Excitation of accelerating wakes in inhomogeneous plasmas", AIP Conf. Proc. vol. 351, Sessler Symposium, pp. 24-48, 1995.
- [19] G. Shvets, J. S. Wurtele, T. C. Chiou, T. Katsouleas, this issue.
- [20] T. Katsouleas, C. Joshi, J.M. Dawson, F.F. Chen, C.E. Clayton, W.B. Mori, C. Darrow, and D. Umstadter, "Plasma accelerators", in *Laser Acceleration of Particles*, edited by C. Joshi and T. Katsouleas, AIP Conf. Proc. vol. 130, pp. 63-98, 1985.
- [21] N.E. Andreev, L.M. Gorbunov, V.I. Kirsanov, A.A. Pogosova and R.R. Ramazashvili, "Resonant excitation of wakefields by a laser pulse in a plasma", *JETP Lett.*, vol. 55, pp. 571-576, 1992 [*Pis'ma Zh. Eksp. Teor. Fiz.*, vol. 55, pp. 551-555, 1992].
- [22] N.E. Andreev, L.M. Gorbunov, V.I. Kirsanov, A.A. Pogosova, and R.R. Ramazashvili, "The Theory of Self-Resonant Wake Field Excitation", *Physica Scripta*, V.49, pp.101-109, 1994.

[23] N.E. Andreev, L.M.Gorbunov, V.I.Kirsanov, and A.A.Pogosova, "Laser Wakefield Accelerator in a Plasma Pipe with Self-modulation of the Laser Pulse", *Sov. Phys. JETP Letters*, V.60(10), pp.713-717, 1994.

[24] N.E.Andreev, L.M.Gorbunov, and V.I.Kirsanov, "Stimulated Processes And Self-Modulation of Short Intense Laser Pulse in Laser Wake-Field Accelerator", *Phys. Plasmas*, Vol.2 (6), pp.2573-2582, 1995.

[25] *Physicists Desk Reference*, H. L. Anderson, ed. (AIP, New York 1989) p. 56.

[26] C.W. Siders, this issue.

[27] E. Esarey, A. Ting, and P. Sprangle, "Frequency shifts induced in laser pulses by plasma waves," *Phys. Rev. A*, vol. 42 no. 6, pp. 3526-3531, Sep. 1990; Wm. M. Wood, C.W. Siders, and M. C. Downer, "Measurement of Femtosecond Ionization Dynamics of Atmospheric Density Gases by Spectral Blueshifting", *Phys. Rev. Lett.*, vol. 67, no. 25, pp. 3523-3526, Dec. 1991; Wm.M. Wood, C.W. Siders, and M.C. Downer, "Femtosecond growth dynamics of an underdense ionization front measured by spectral blueshifting," *IEEE Trans. Plasma Sci.*, vol. 21, no. 1, pp. 20-33, Feb. 1993.

[28] S. P. Le Blanc, R. Sauerbrey, S.C. Rae, and K. Burnett, "Spectral blue shifting of a femtosecond laser pulse propagating through a high-pressure gas," *J. Opt. Soc. Am. B*, vol. 10, no. 10, pp. 1801-1809, Oct. 1993; S.P. Le Blanc, Z. Qi, and R. Sauerbrey, "Femtosecond vacuum-ultraviolet pulse measurement by field-ionization dynamics," *J. Opt. Soc. Am. B*, vol. 20, no. 3, pp. 312-314, Feb. 1995.

[29] L. Serafini et al., this issue.

[30] P. Sprangle, J. Krall, and E. Esarey, "hose modulation instability of laser pulses in plasmas", *Phys. Rev. Lett.*, vol. 73, pp. 3544, 1994.

[31] J.M. Rax and N. J. Fisch, "Nonlinear relativistic interaction of an ultrashort laser pulse with a cold plasma", Phys. Fluids B, vol. 4, pp 1323, 1992; E. Esarey, G. Joyce, and P. Sprangle, "Frequency upshifting of laser pulses by copropagating ionization fronts", Phys. Rev. A, vol. 44, pp. 3908, 1991.

[32] E. Esarey and J. Krall (to be published).

[33] W.B. Mori, C. Decker, D.E. Hinkel, T. Katsouleas, "Raman forward scattering of short pulse high intensity lasers", Phys. Rev. Lett., vol. 72, pp. 1482 - 1485, 1994.

[34] C.D. Decker, W.B. Mori, "Group velocity of large amplitude electromagnetic waves in a plasma", Phys. Rev. Lett., vol. 72, pp. 490 - 493, 1994.

Figure Captions

Fig. 1: Parametric plot for laser systems for second generation guiding and wakefield excitation experiments. The bottom horizontal axis is the laser pulse length (in fs) which is directly proportional to γ_g for a Gaussian laser pulse shape. The top horizontal axis is the dephasing length (in cm) and the resonant plasma density, again for a Gaussian pulse shape. The vertical axis on the left is the energy per pulse. The vertical axis on the right are the laser system maximum repetition rate (in Hz) and the minimum required diameter of the final laser amplifier (in cm) to stay below the damage fluence level of 2 J/cm^2 . The dashed lines are constant laser power lines. The shaded area is delineated from the left by the line $P = P_{\text{crit}}$ and from the right by $E_z = 1 \text{ GeV/m}$, and seems, at the present, to be the optimum regime for second generation experiments.

Fig. 2: Same as Fig. 1 but superimposed are iso-energy gain lines in a laser wakefield experiment with an acceleration distance equal to πZ_R (i.e. without optical guiding).

Fig. 3: Same as Fig. 1 but superimposed are iso-energy gain lines in a laser wakefield experiment with an acceleration distance equal to the dephasing length (i.e. with optical guiding).

Fig. 4: Numerical simulation of the wakefield excitation by short laser pulses in parabolic channels for the cases A and B (see Table 2). The normalized maximum of the wake amplitude ($\delta n / n_0$) (upper plots) and the maximum of the laser field amplitude (a_0) (lower plots) on the plasma channel axis ($r=0$) are plotted as function of the laser pulse propagation length z / Z_R for the cases A and B (left and right plots). Dashed lines on the upper plots indicate the results of 1-D theory for the wake amplitude (see Eq.(7-9) at $k_p r_s \gg 1$).

Fig. 5: Schematic of a low intensity, initially uniform, guided laser beam propagating in the presence of an externally generated plasma wave. The plasma wave produces periodic regions of enhanced focusing and enhanced diffraction, thus modulating the laser beam such that the intensity maxima are in phase with the density minima.

Fig. 6: Numerical simulation of self-modulation in a long flattop laser pulse. The initial axial intensity profile is zero at $\zeta = 0$ and rises to $a_0 = 0.028$ at $\zeta = -5\lambda_p$, followed by a long flattop region with $a_0 = 0.028$ for $\zeta < -5\lambda_p$. The flattop region of the pulse is primarily channel guided with $\Delta n / \Delta n_c = 0.9$, $P/P_c = 0.1$, $n_0 = 1.24 \times 10^{16} \text{ cm}^{-3}$ ($\lambda_p = 300 \text{ } \mu\text{m}$), $r_0 = 0.3 \text{ cm}$, and $\lambda = 1 \text{ } \mu\text{m}$. The normalized intensity modulation $\delta a^2 / a_0^2$ (dashed line), where $\delta a^2 = a^2 - a_0^2$, and the normalized plasma density wave $\delta n / n_0$ (solid line), are plotted as a function of ζ / λ_p after propagating a distance $z = 6.4 Z_R$ in Fig. 6(a) and $z = 8.0 Z_R$ in Fig. 6(b).

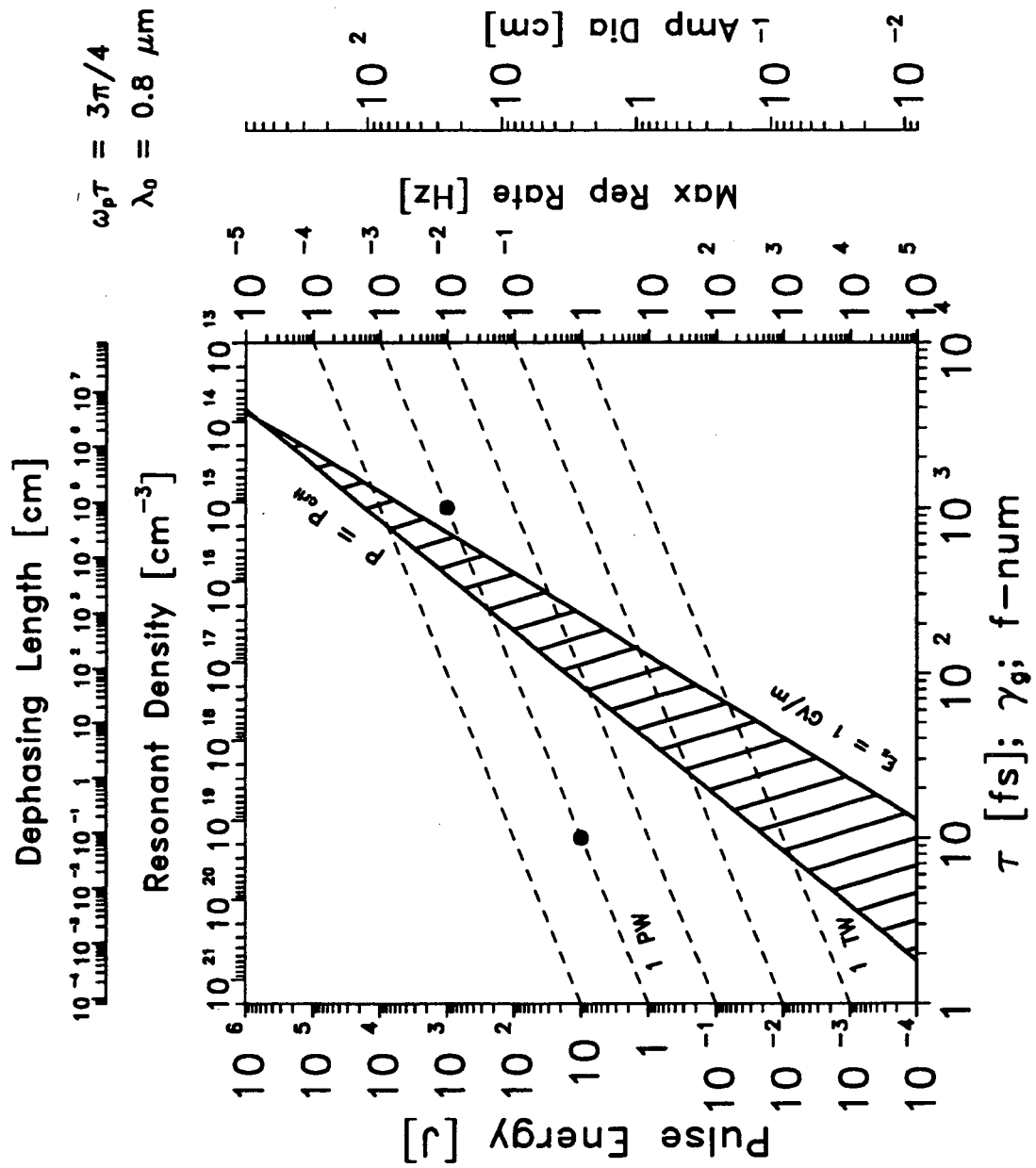


Fig. 1

Fig. 2

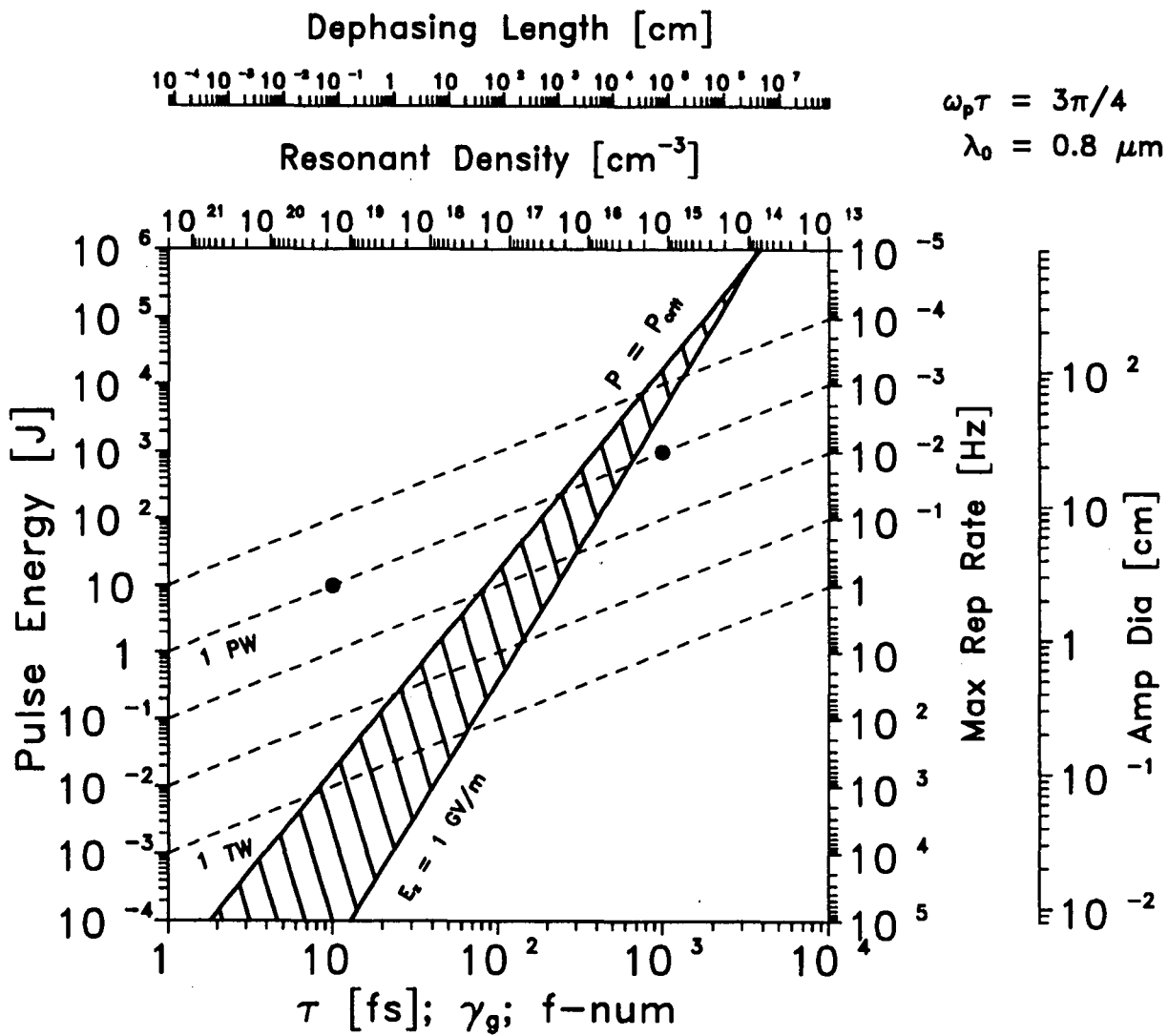


Fig. 3

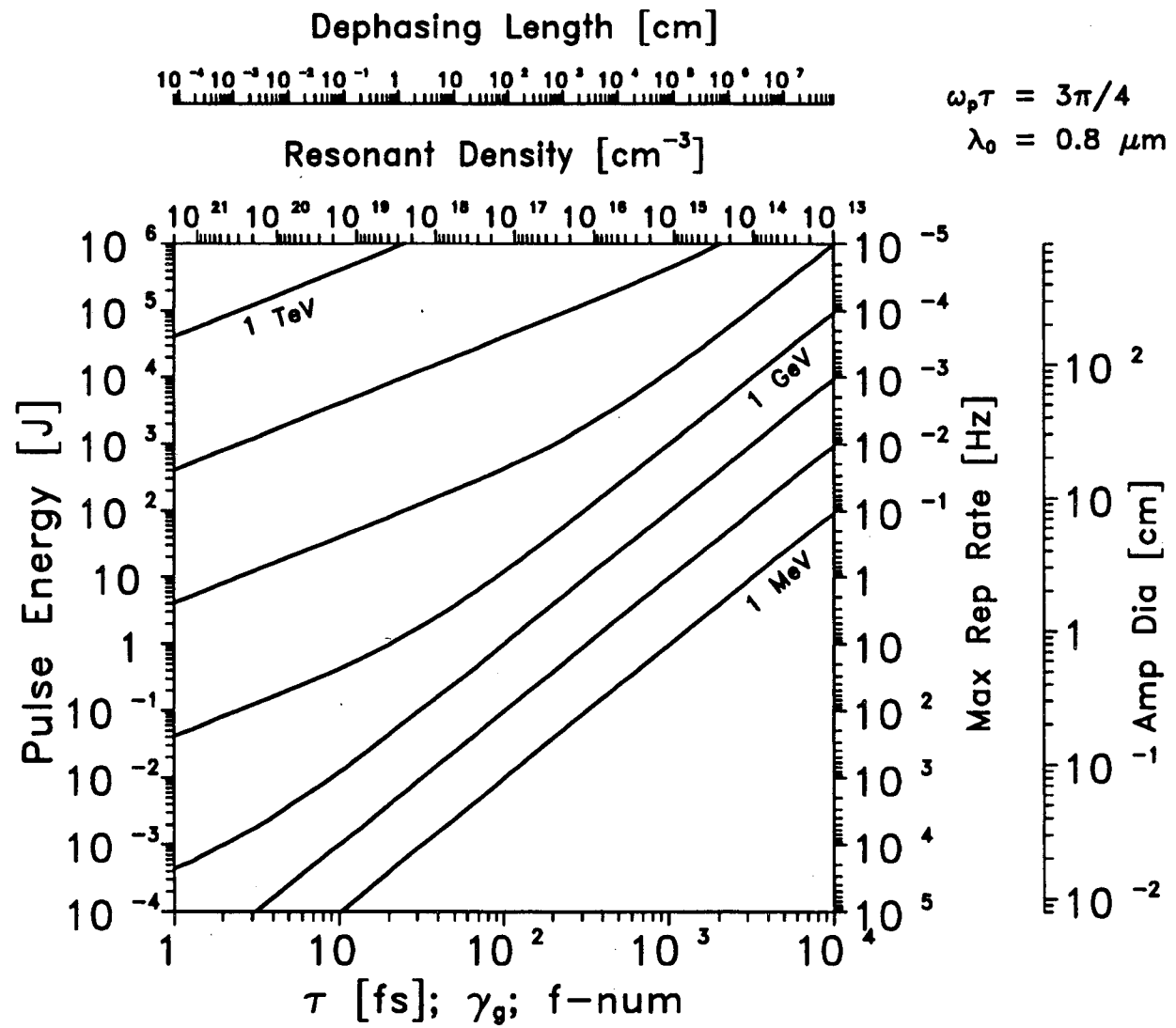
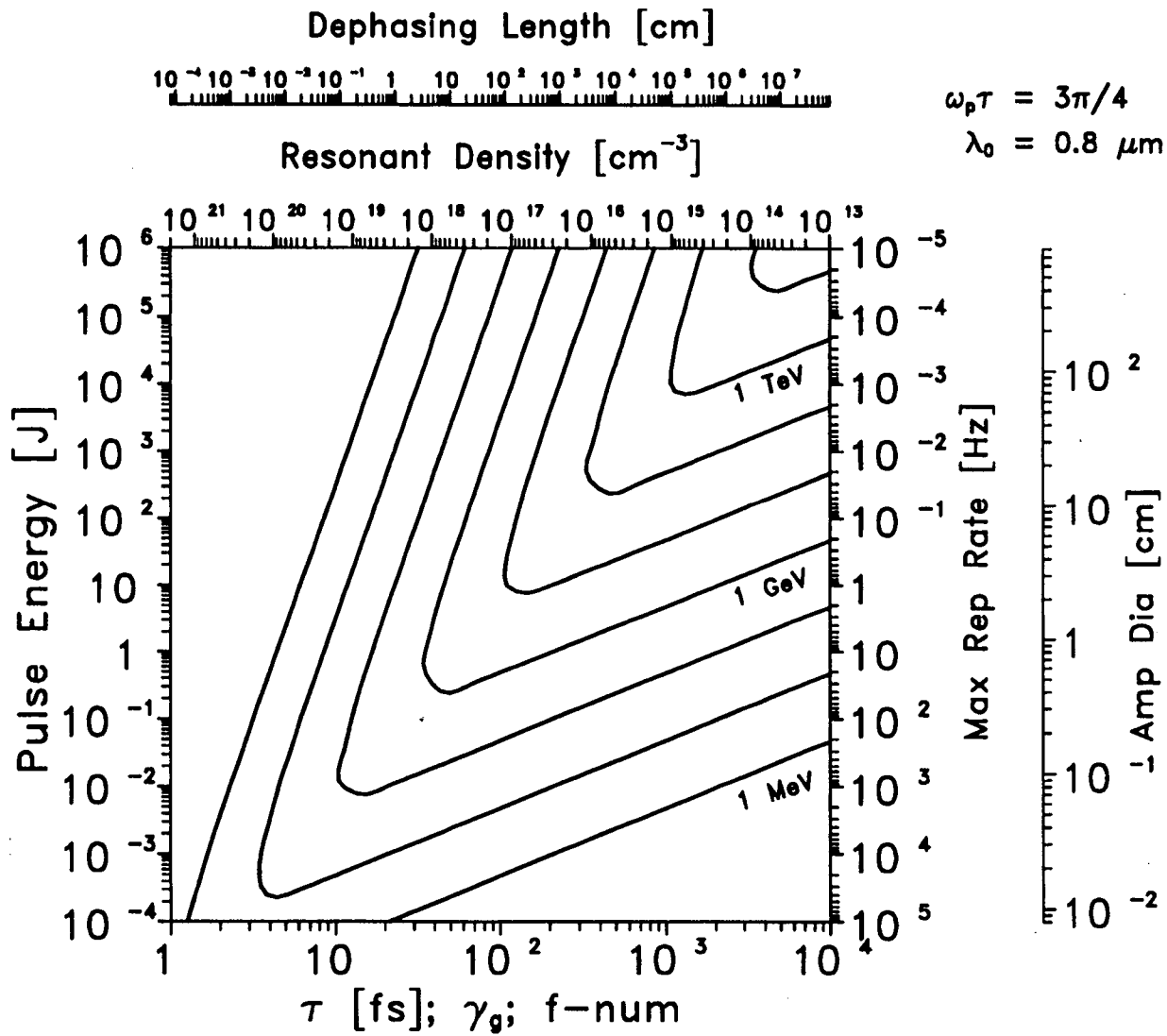


Fig. 4



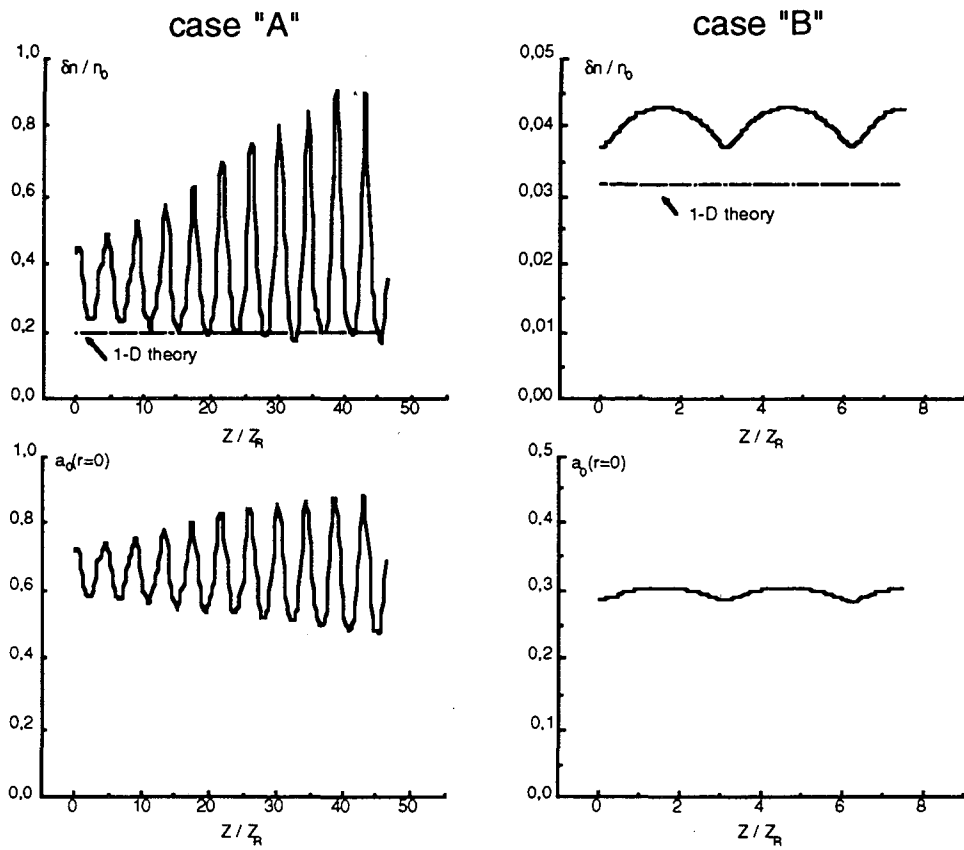


Fig. 5

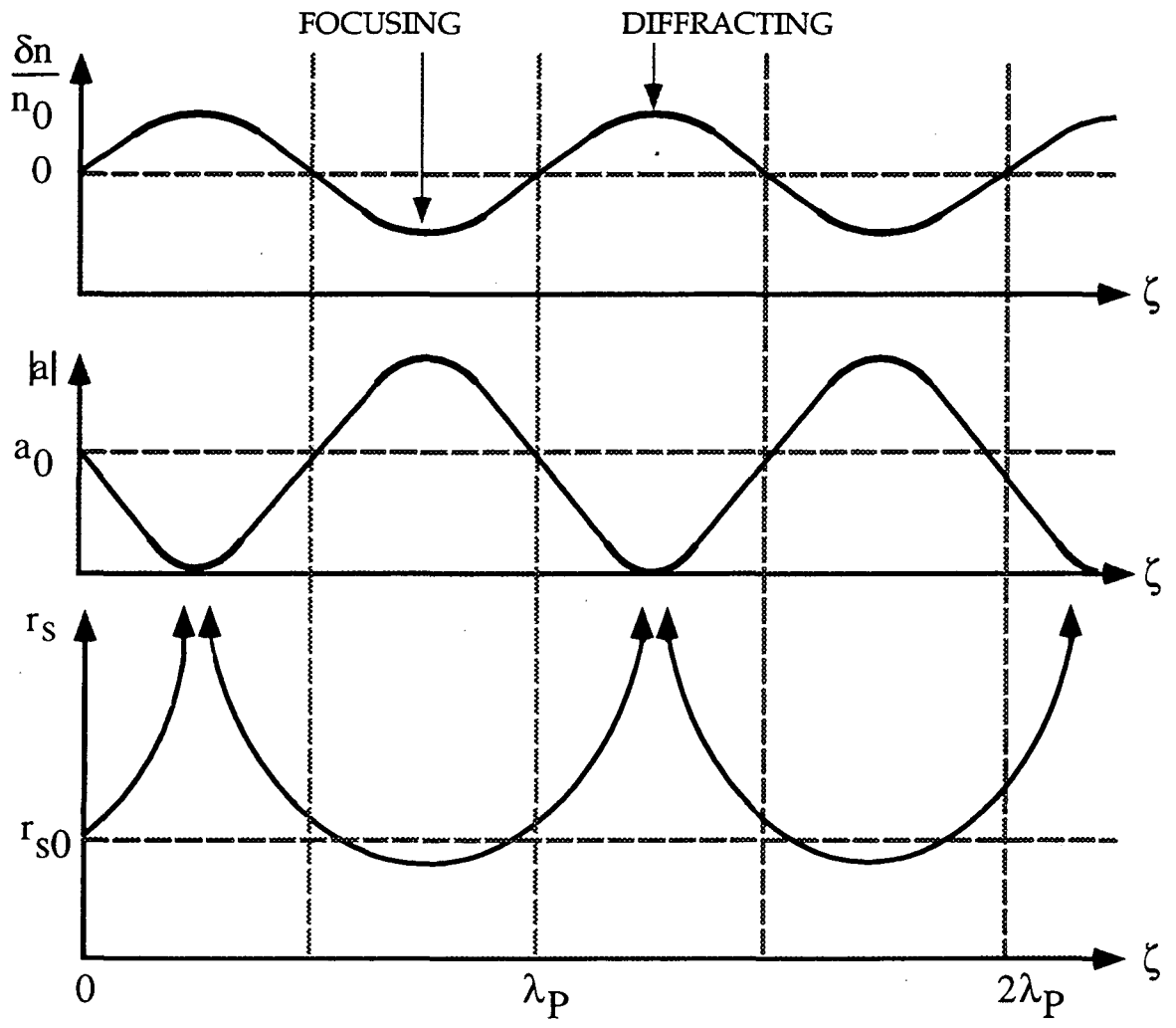


Fig. 6

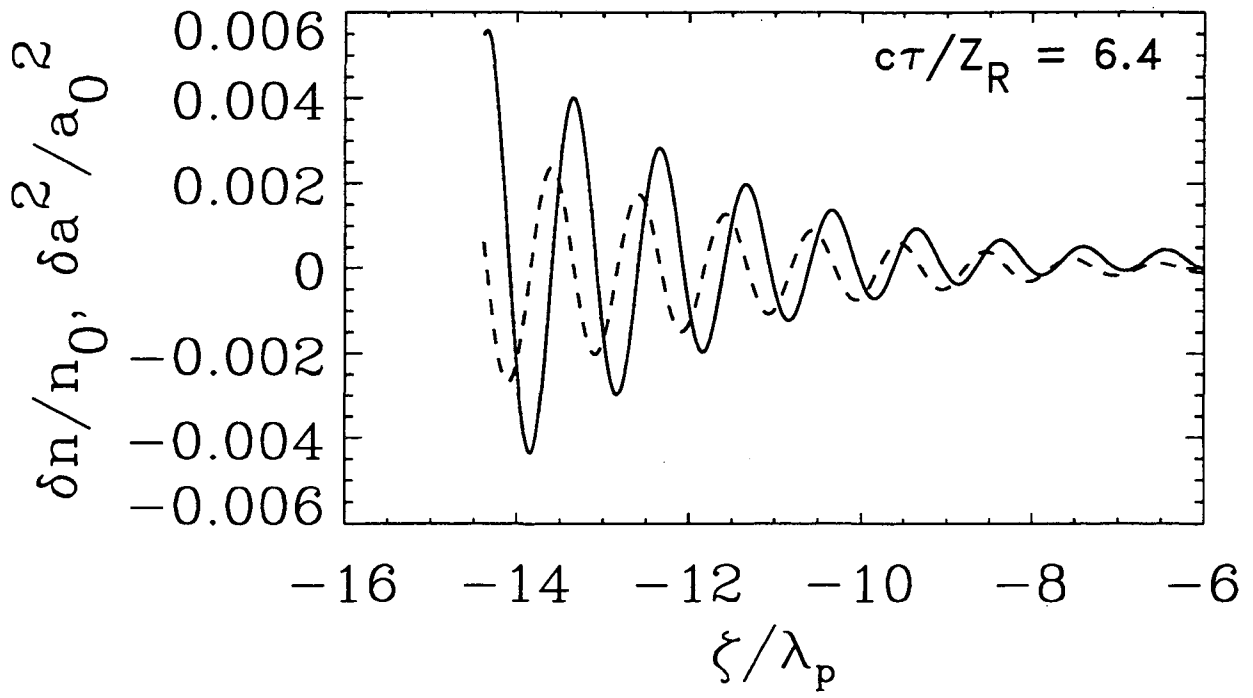


Fig. 6(a)

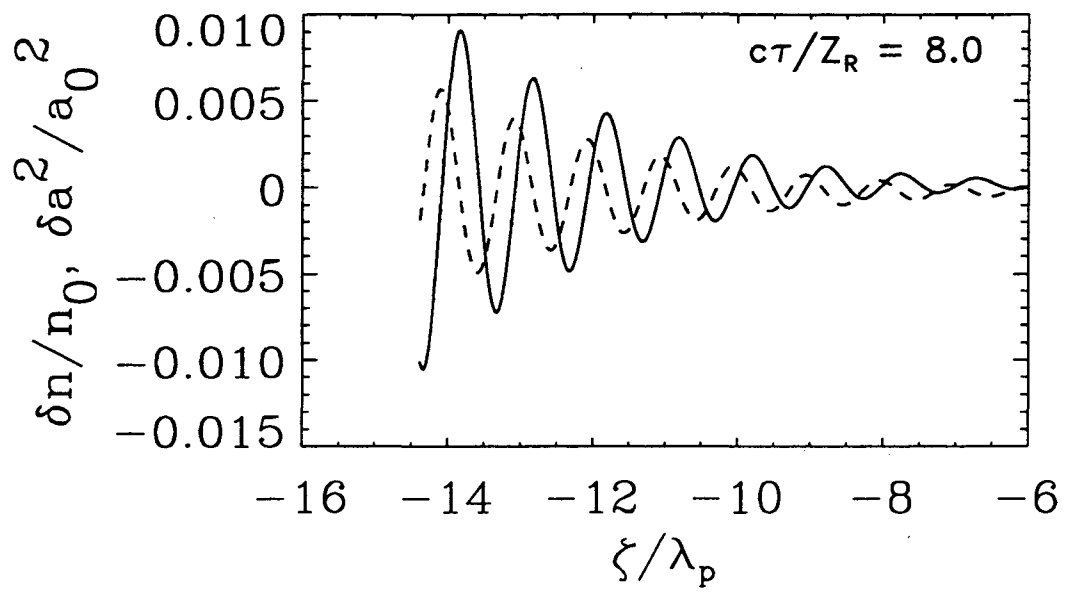


Fig. 6(b)

**ERNEST ORLANDO LAWRENCE BERKELEY NATIONAL LABORATORY
ONE CYCLOTRON ROAD | BERKELEY, CALIFORNIA 94720**